

# Understanding the microwave dielectric properties of $(\text{Pb}_{0.45}\text{Ca}_{0.55})[\text{Fe}_{0.5}(\text{Nb}_{1-x}\text{Ta}_x)_{0.5}]\text{O}_3$ ceramics via the bond valence

Ki Hyun Yoon<sup>a,\*</sup>, Eung Soo Kim<sup>b</sup>, Jong-Suk Jeon<sup>b</sup>

<sup>a</sup>Department of Ceramic Engineering, Yonsei University, Seoul 120-749, South Korea

<sup>b</sup>Department of Materials Engineering, Kyonggi University, Suwon 442-760, South Korea

## Abstract

Microwave dielectric properties of the  $(\text{Pb}_{0.45}\text{Ca}_{0.55})[\text{Fe}_{0.5}(\text{Nb}_{1-x}\text{Ta}_x)_{0.5}]\text{O}_3$  ceramics were investigated in the range of  $0.0 \leq x(\text{mol}) \leq 1.0$ . With increasing  $\text{Ta}_2\text{O}_5$ , the dielectric constant and the temperature coefficient of the resonant frequency (TCF) decreased, while the  $Q:f$  value of the specimens increased. The change of dielectric constant was evaluated by the correlation between ionic polarizability and bond valence. TCF of the specimens decreased with the tilting of oxygen octahedra due to an increase of bond valence of the B-site. The  $Q:f$  values were studied by infrared reflectivity spectra from 50 to  $4000\text{ cm}^{-1}$ , and calculated by the Kramers-Kronig analysis and classical oscillator model. The specimens with 0.4 mol of  $\text{Ta}_2\text{O}_5$  sintered at  $1150\text{ }^\circ\text{C}$  for 3 h showed  $\epsilon_r$  of 82,  $Q:f$  of 7650, and TCF of  $-5\text{ ppm}/^\circ\text{C}$ .

© 2003 Elsevier Ltd. All rights reserved.

**Keywords:** Bond valence; Ionic polarizability; IR reflectivity; Microwave ceramics; Dielectric properties;  $(\text{PbCa})\text{Fe}(\text{NbTa})\text{O}_3$

## 1. Introduction

It is well known that the dielectric materials available to the microwave devices should have predictable properties with a high dielectric constant ( $K$ ), a high loss quality ( $Q:f$ ), and a small temperature coefficient of the resonant frequency (TCF). Various dielectric materials have been investigated to develop their microwave dielectric properties and to satisfy these requirements. However, a fundamental relationship between the structural characteristics and the dielectric properties should be studied to help control their dielectric properties.

The dielectric properties are largely affected by the structural characteristics of the solid solution. Since the bond valence is a function of bond strength and bond length,<sup>1</sup> the structural characteristics are largely depended on the bond valence. Therefore, the dielectric properties can effectively be estimated by bond valence. Moreover, far-infrared spectra measurement of the dielectric materials or solid solution is known as a useful

method to understand the dielectric constant and dielectric loss mechanism at microwave frequencies.<sup>2</sup>

Recently, microwave dielectric materials with a high dielectric constant and a low sintering temperature have become required to meet the demand for the miniaturization of microwave devices. Several kinds of materials have been investigated to meet these requirements and the promising candidates are the Pb-based complex perovskite compounds. According to Kato et al.,<sup>3</sup> the dielectric constant decreases with the decrease of the B-site ionic radius of in the  $(\text{Pb,Ca})(\text{Me,Nb})\text{O}_3$  system. However, other reports showed different results. When Ti with the smaller ionic size ( $0.61\text{ \AA}$ , CN=6) than the average ionic size of B-site (Fe,Nb) ( $0.64\text{ \AA}$ ), was substituted for the B-site (Fe,Nb) of  $(\text{Pb,Ca})(\text{Fe,Nb})\text{O}_3$ , the dielectric constant increased.<sup>4</sup> While, the substitution of larger ionic size Sn ( $0.69\text{ \AA}$ , CN=6) showed a decrease of dielectric constant.<sup>5</sup>

Therefore, the effect of bond valence on the microwave dielectric properties of the  $(\text{Pb}_{0.45}\text{Ca}_{0.55})[\text{Fe}_{0.5}(\text{Nb}_{1-x}\text{Ta}_x)_{0.5}]\text{O}_3$  ceramics have been investigated as a function of the substitution of  $\text{Ta}_2\text{O}_5$  content ( $0.0 \leq x \leq 1.0$ ). Far-infrared reflectivity spectra of the specimens were also investigated to evaluate the intrinsic dielectric loss with the structural change.

\* Corresponding author. Tel.: +82-2-2123-2848; fax: +82-2-392-1680.

E-mail address: khyoon@yonsei.ac.kr (K.H. Yoon).

## 2. Experimental procedure

PbO, CaCO<sub>3</sub>, Fe<sub>2</sub>O<sub>3</sub>, Nb<sub>2</sub>O<sub>5</sub> and Ta<sub>2</sub>O<sub>5</sub> powders with high-purity (>99.9%) were used as starting materials. They were weighed according to the compositions of (Pb<sub>0.45</sub>Ca<sub>0.55</sub>)[Fe<sub>0.5</sub>(Nb<sub>1-x</sub>Ta<sub>x</sub>)<sub>0.5</sub>]O<sub>3</sub> (0.0 ≤ x ≤ 1.0), and then milled with ZrO<sub>2</sub> balls for 24 h in distilled water. The mixtures were dried and calcined at 900 °C for 4 h, and then pressed into 10 mm diameter disks under a pressure of 1500 kg/cm<sup>2</sup> isostatically. These disks were sintered at 1150 °C for 3 h in air. Burying the specimens in powders of the same compositions and placing them into a platinum crucible inhibited the loss of PbO and decomposition during the sintering process.<sup>6</sup>

X-ray powder diffraction analysis (D/Max-3C, Rigaku, Japan) was used to determine the crystalline structure and lattice parameters. The polished surface was observed using a scanning electron microscope (JEOL, JSM 820, Japan). The dielectric constant and unloaded *Q* value at frequencies of 5–6 GHz were measured by the post resonator method developed by Hakki and Coleman. TCF was measured by the cavity method at frequencies of 9–11 GHz and the temperature range of 25–80 °C. The reflectivity spectra were measured using a Fourier-transform infrared spectrometer (Model DA-8.12, Bomen, Inc., Toronto, Canada) from 50 to 4000 cm<sup>-1</sup>. The polished samples were set in a vacuum chamber evacuated to 0.3 torr and the reflectivity spectra were obtained relative to the reflectivity of the gold mirror. The spectra were recorded at a resolution of 4 cm<sup>-1</sup>. The incident angle of radiation was 7°.

The observed dielectric polarizability ( $\alpha_{\text{obs.}}$ ) of the specimens were obtained from measured dielectric constant and the unit-cell volume using the Clausius-Mosotti equation. The theoretical dielectric polarizability ( $\alpha_{\text{theo.}}$ ) of the specimens were calculated from the ionic polarizabilities of component ions and the additive rule of dielectric polarizabilities.<sup>7,8</sup> The bond valence of the B-site in ABO<sub>3</sub> perovskite was calculated from the bond valence parameters of the B-site cation and the distance ( $d_{\text{B-O}}$ ) between B-site cation and oxygen.<sup>1</sup>

## 3. Results and discussion

Fig. 1 shows X-ray diffraction patterns of (Pb<sub>0.45</sub>Ca<sub>0.55</sub>)[Fe<sub>0.5</sub>(Nb<sub>1-x</sub>Ta<sub>x</sub>)<sub>0.5</sub>]O<sub>3</sub> (0.0 ≤ x ≤ 1.0, PCFNT) ceramics sintered at 1150 °C for 3 h. In the entire compositional range, a single phase with cubic perovskite (Pm3m) was detected, because Ta<sup>5+</sup> ion was easily substituted for Nb<sup>5+</sup> ion due to the same effective ionic radius of 0.64 Å at a coordination number of six. Also, the lattice parameter of the specimens showed nearly same value.

Fig. 2 shows SEM micrographs of PCFNT ceramics sintered at 1150 °C for 3 h. With an increase of Ta<sup>5+</sup>

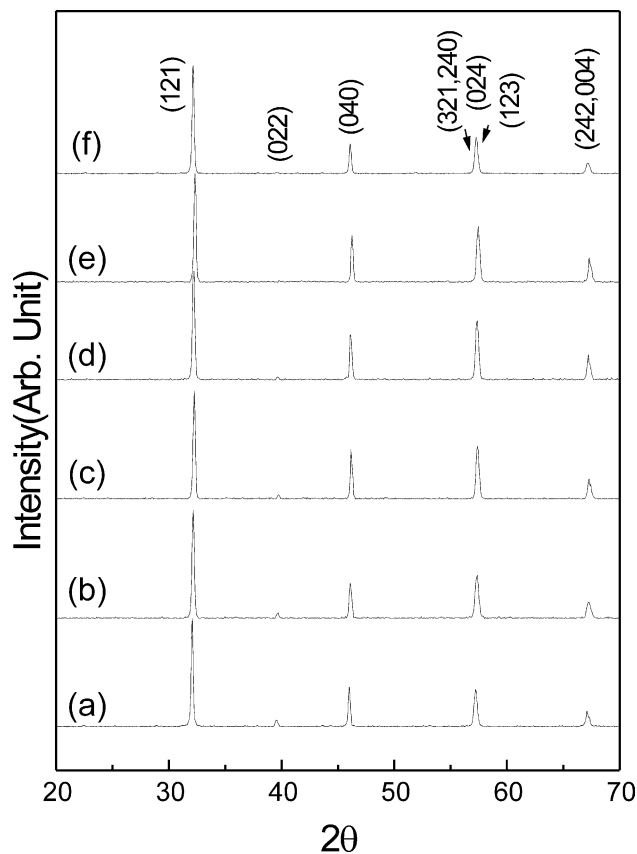


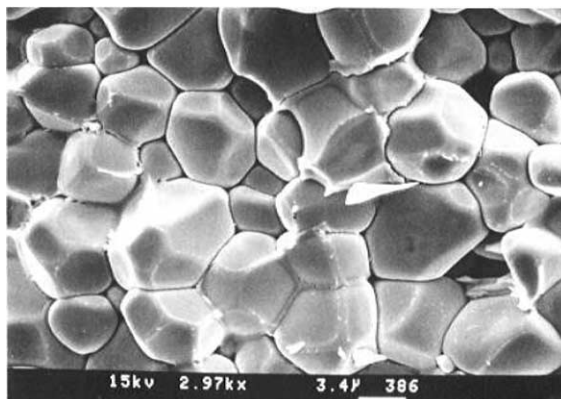
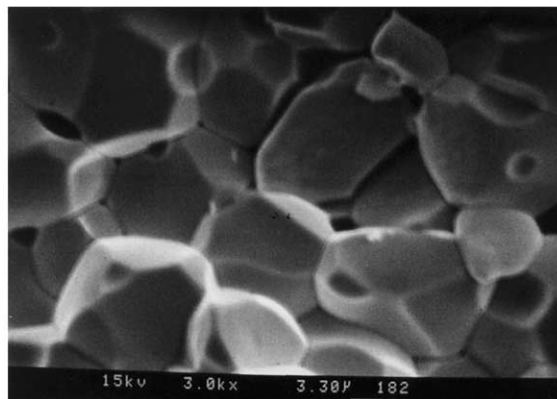
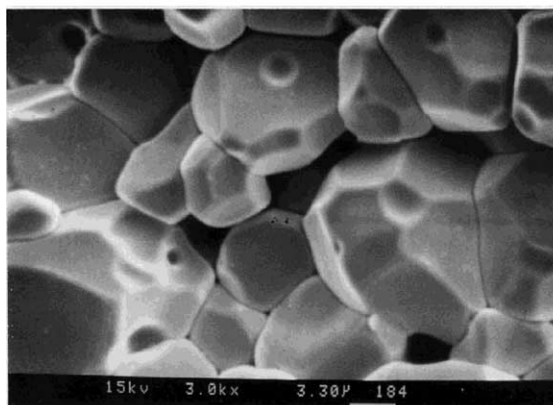
Fig. 1. X-ray diffraction patterns of (Pb<sub>0.45</sub>Ca<sub>0.55</sub>)[Fe<sub>0.5</sub>(Nb<sub>1-x</sub>Ta<sub>x</sub>)<sub>0.5</sub>]O<sub>3</sub> specimens sintered at 1150 °C for 3 h; (a) *x* = 0, (b) *x* = 0.2, (c) *x* = 0.4, (d) *x* = 0.6, (e) *x* = 0.8, and (f) *x* = 1.0.

content, grain size was significantly increased. Therefore, the grain growth was enhanced by the substitution of Ta<sup>5+</sup> for Nb<sup>5+</sup>.

With an increase of Ta<sup>5+</sup> content, the dielectric constant decreased, as shown in Fig. 3. The dielectric constant was largely depended on the relative density and ionic polarizability at microwave frequencies. Since the relative densities of PCFNT specimens were higher than 96%, the dielectric constant was not significantly affected by the relative density,<sup>9</sup> so that the ionic polarizability was the more important factor affecting the dielectric constant. Table 1 shows the ionic polarizability of PCFNT specimens sintered at 1150 °C for 3 h. With an increase of Ta<sup>5+</sup> content, the theoretical ionic polarizabilities ( $\alpha_{\text{theo.}}$ ) obtained from the additive rule increased due to the larger ionic polarizability of Ta<sup>5+</sup> (4.73 Å<sup>3</sup>) than Nb<sup>5+</sup> (3.97 Å<sup>3</sup>). Even though theoretical ionic polarizability increased with an increase of Ta<sup>5+</sup> content, the dielectric constant of the specimens decreased. These results are due to the decrease of rattling effect, which could be estimated by the deviation of  $\alpha_{\text{theo.}}$  from derived ionic polarizability ( $\alpha_{\text{der.}}$ ) obtained from the measured dielectric constants using the

Clausius-Mosotti equation.<sup>7</sup> The B-site bond valence increased with an increase of Ta<sup>5+</sup> content, as shown in Table 2. Since both the bond valence and rattling effect are a function of bond strength, the rattling effect, and, in turn, the deviation of  $\alpha_{\text{der.}}$  from  $\alpha_{\text{theo.}}$  depended on bond valence, as shown in Fig. 4. Therefore, the dielectric constant of PCFNT specimens decreased with an increase of Ta<sup>5+</sup> content due to the increase of B-site bond valence.

The temperature coefficient of resonant frequency (TCF) is a function of the linear thermal expansion coefficient ( $\alpha_L$ ) and the temperature coefficient of dielectric constant (TCK).<sup>10</sup> In the ceramics, the magnitude of  $\alpha_L$  could be taken as a constant about 10 ppm/°C, so that TCF directly depended on TCK. Although the tilting of oxygen octahedra has been reported to be closely related to the tolerance factor and TCK,<sup>11,12</sup> the oxygen octahedra was more closely related to the bond

(a)  $x=0.2$ (b)  $x=0.4$ (c)  $x=0.8$ 

—  
5  $\mu\text{m}$

Fig. 2. SEM micrographs of  $(\text{Pb}_{0.45}\text{Ca}_{0.55})[\text{Fe}_{0.5}(\text{Nb}_{1-x}\text{Ta}_x)_{0.5}]\text{O}_3$  specimens sintered at 1150 °C for 3 h; (a)  $x=0.2$ , (b)  $x=0.4$  and (c)  $x=0.8$ .

Table 1

Comparison of theoretical and derived ionic polarizability of  $(\text{Pb}_{0.45}\text{Ca}_{0.55})[\text{Fe}_{0.5}(\text{Nb}_{1-x}\text{Ta}_x)_{0.5}]\text{O}_3$  specimens sintered at 1150 °C for 3 h

$x$ (mol)	Theoretical $\alpha_{\text{theo.}}$	Derived				$\Delta, \% (\alpha_{\text{der.}} - \alpha_{\text{theo.}}) / \alpha_{\text{der.}} \times 100$
		$K$	$V_{\text{unit-cell}}$	$Z$	$\alpha_{\text{der.}}$	
0	13.8590	92.8	61.256	1	14.1609	2.13
0.2	13.9350	84.0	61.037	1	14.0633	0.91
0.4	14.0110	83.0	61.004	1	14.0497	0.28
0.6	14.0870	80.0	61.032	1	14.0374	−0.35
0.8	14.1630	72.9	61.097	1	14.0020	−1.15
1.0	14.2390	69.2	61.162	1	13.9859	−1.81

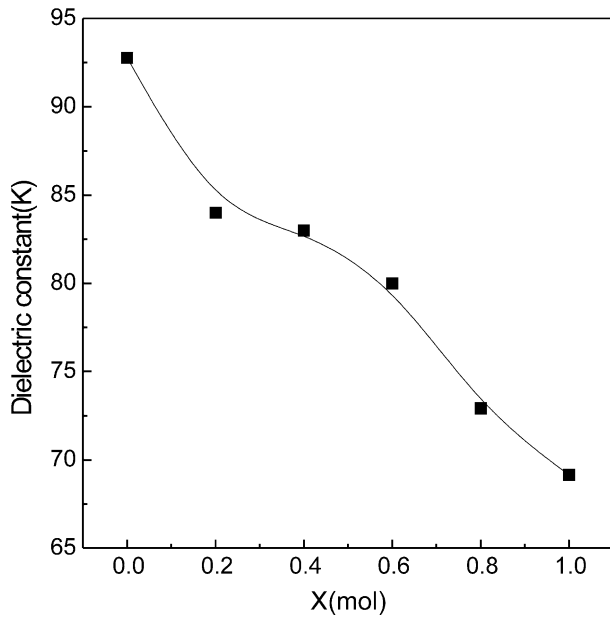


Fig. 3. Dielectric constant of  $(\text{Pb}_{0.45}\text{Ca}_{0.55})[\text{Fe}_{0.5}(\text{Nb}_{1-x}\text{Ta}_x)_{0.5}]\text{O}_3$  specimens sintered at  $1150^\circ\text{C}$  for 3 h.

Table 2

B-site bond valence (VB) of  $(\text{Pb}_{0.45}\text{Ca}_{0.55})[\text{Fe}_{0.5}(\text{Nb}_{1-x}\text{Ta}_x)_{0.5}]\text{O}_3$  specimens sintered at  $1150^\circ\text{C}$  for 3 h

$x$ (mol)	$a$ (Å)	$R_{\text{Fe,Nb,Ta-O}}$	$d_{\text{Fe,Nb,Ta-O}}$	$b$	$V_{\text{Fe,Nb,Ta-O}}$	TCF (ppm/ $^\circ\text{C}$ )
0	3.9420	1.8350	1.9710	0.37	4.1545	2.69
0.2	3.9373	1.8359	1.9686	0.37	4.1912	-4.67
0.4	3.9366	1.8368	1.9683	0.37	4.2053	-5.66
0.6	3.9372	1.8377	1.9686	0.37	4.2122	-7.33
0.8	3.9386	1.8386	1.9693	0.37	4.2144	-12.42
1.0	3.9400	1.8395	1.9700	0.37	4.2167	-14.5

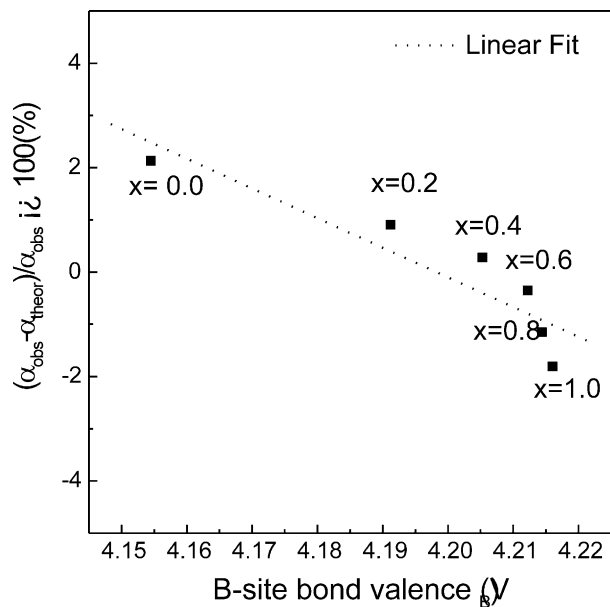


Fig. 4. Deviation from ionic polarizability and B-site bond valence of  $(\text{Pb}_{0.45}\text{Ca}_{0.55})[\text{Fe}_{0.5}(\text{Nb}_{1-x}\text{Ta}_x)_{0.5}]\text{O}_3$  specimens sintered at  $1150^\circ\text{C}$  for 3 h.

length and bond strength between the cation in the octahedral site and the oxygen than the ionic radius. Therefore, the tilting of oxygen octahedra and TCF could be more effectively estimated by the B-site bond valence than the tolerance factor in  $\text{ABO}_3$  complex perovskites.<sup>13</sup> Even though the tolerance factor was a constant value of 0.9719 throughout the entire compositional range, TCF was decreased with an increase of  $\text{Ta}^{5+}$  content. These results are due to an increase of the B-site bond valence. The dependence of TCF on the B-site bond valence is shown in Fig. 5.

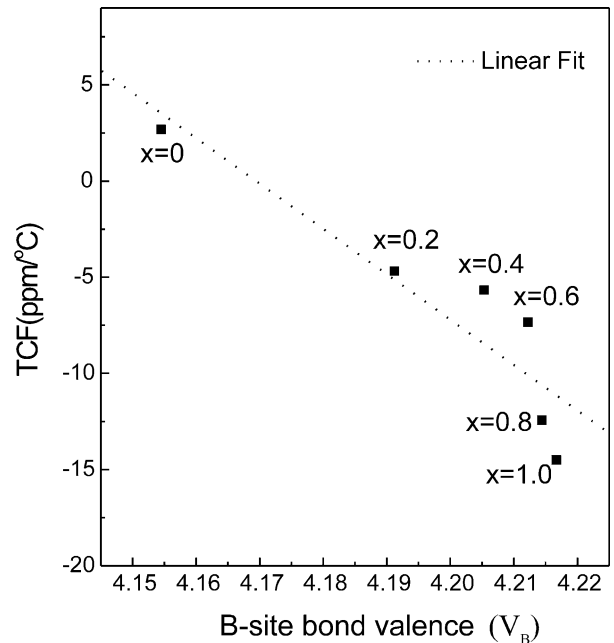


Fig. 5. TCF and B-site bond valence of  $(\text{Pb}_{0.45}\text{Ca}_{0.55})[\text{Fe}_{0.5}(\text{Nb}_{1-x}\text{Ta}_x)_{0.5}]\text{O}_3$  specimens sintered at  $1150^\circ\text{C}$  for 3 h.

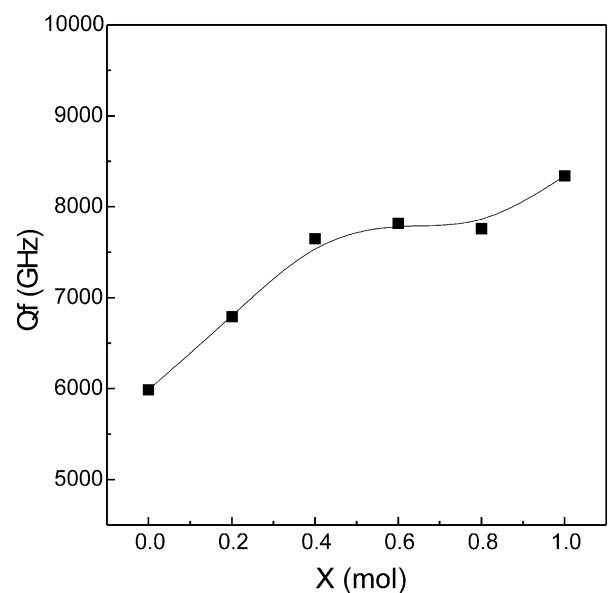


Fig. 6. Quality factor ( $Qf$ ) of  $(\text{Pb}_{0.45}\text{Ca}_{0.55})[\text{Fe}_{0.5}(\text{Nb}_{1-x}\text{Ta}_x)_{0.5}]\text{O}_3$  specimens sintered at  $1150^\circ\text{C}$  for 3 h.

Table 3

Dispersion parameters of  $(\text{Pb}_{0.45}\text{Ca}_{0.55})[\text{Fe}_{0.5}(\text{Nb}_{1-x}\text{Ta}_x)_{0.5}]\text{O}_3$  specimens obtained from the best fit to the reflectivity data

$j$	$x=0$				$x=0.2$				$x=0.4$				$x=0.8$				$x=1.0$			
	$\Omega_j$ ( $\text{cm}^{-1}$ )	$\gamma_j$ ( $\text{cm}^{-1}$ )	$\Delta\varepsilon_j$	$\tan \delta_j$ ( $\times 10^{-4}$ )	$\Omega_j$ ( $\text{cm}^{-1}$ )	$\gamma_j$ ( $\text{cm}^{-1}$ )	$\Delta\varepsilon_j$	$\tan \delta_j$ ( $\times 10^{-4}$ )	$\Omega_j$ ( $\text{cm}^{-1}$ )	$\gamma_j$ ( $\text{cm}^{-1}$ )	$\Delta\varepsilon_j$	$\tan \delta_j$ ( $\times 10^{-4}$ )	$\Omega_j$ ( $\text{cm}^{-1}$ )	$\gamma_j$ ( $\text{cm}^{-1}$ )	$\Delta\varepsilon_j$	$\tan \delta_j$ ( $\times 10^{-4}$ )	$\Omega_j$ ( $\text{cm}^{-1}$ )	$\gamma_j$ ( $\text{cm}^{-1}$ )	$\Delta\varepsilon_j$	$\tan \delta_j$ ( $\times 10^{-4}$ )
1	70	36.5	44.3	6.1827	70.212	35	38	4.6075	71.369	36	35.2	4.3595	72	37	27.25	3.9871	69.94	28	23.03	3.963
2	93.139	14.42	3.33	0.1013	96.411	25	3	0.1572	90.011	6.902	0.38	0.0066	98.319	36	7	0.6128	92.981	48	8	0.488
3	104.49	14.42	2.7	0.0603	108.59	14	0.69	0.4902	104.77	34.79	8.12	0.4880	116	38.48	4.87	0.3230	103.73	31.12	4.58	0.3839
4	124.01	32.46	8.5	0.2771	122.33	55	8	0.5730	139.46	55	8	0.5730	139.65	41.20	5.05	0.2473	126.87	46.03	4.95	0.4102
5	149.89	38.37	4.77	0.1475	152.13	20	2	0.1779	156.44	50	2	0.0157	158.2	21.09	1.15	0.0224	138.78	40.95	0.9	0.0556
6	168.29	30.38	1.14	0.0222	166.71	17	0.7	0.0054	173.1	18	0.7	0.0054	171.6	15	1	0.007	163.06	44.00	4.13	0.1983
7	206.25	50	20	0.4021	209.27	50	17.9	0.3012	210.07	37	17.9	0.3012	209.64	35.5	16	0.2761	208.43	32	12.8	0.2644
8	272.07	69	1.8	0.0258	267.32	78	2	0.0361	257.88	66.64	2	0.0361	253.49	68.29	2.5	0.0426	224.53	75.05	3.5	0.1468
9	326.51	40	0.4	0.0034	320.52	45	0.75	0.0091	304.89	44.13	0.75	0.0091	300	45.19	1.12	0.0130	293.61	48.19	1.5	0.0225
10	552.31	48.21	1.25	0.0033	557.48	43.41	1.52	0.0041	566.26	43.15	1.52	0.0041	569.54	45.76	1.5	0.0045	573.28	45.47	1.31	0.0052
11	577.04	51.29	0.59	0.0492	578.96	50.21	0.23	0.0005	586.34	38.72	0.23	0.0005	593.1	45.72	0.16	0.0004	579.39	46.51	0.14	0.0005
12	724.61	76.7	0.06	0.001	724.87	78.91	0.05	0.0001	728.76	67.26	0.05	0.0001	728.29	70.38	0.05	0.0001	729.04	71.92	0.05	0.0001
	$\varepsilon_\infty = 5.06$				$\varepsilon_\infty = 4.77$				$\varepsilon_\infty = 4.62$				$\varepsilon_\infty = 4.53$				$\varepsilon_\infty = 4.41$			

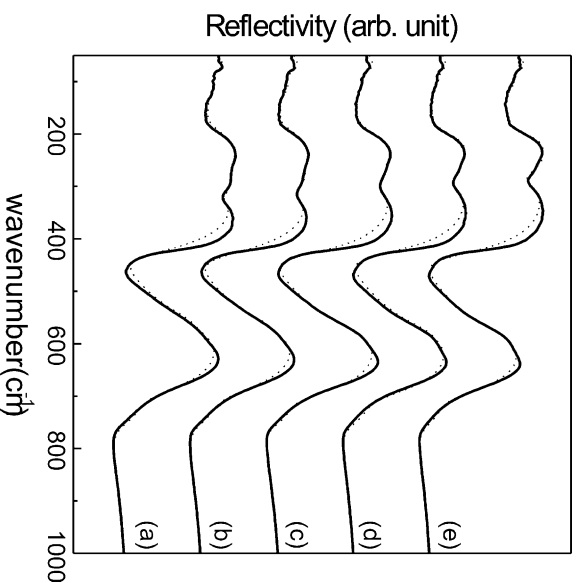
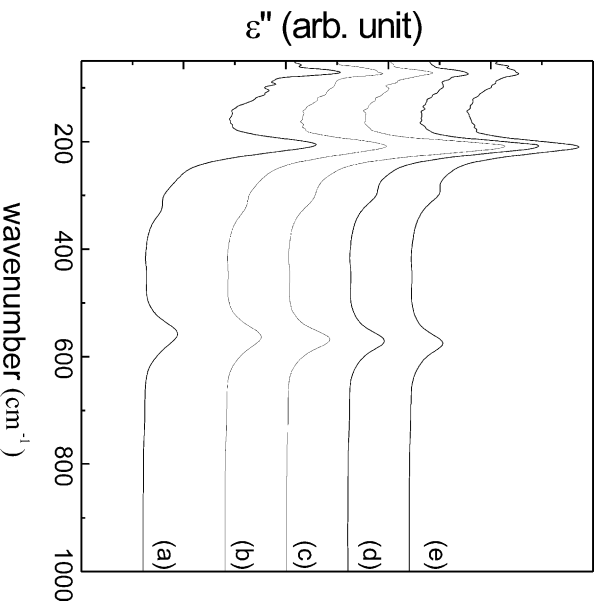
Fig. 7. Infrared reflectivity spectra of  $(\text{Pb}_{0.45}\text{Ca}_{0.55})[\text{Fe}_{0.5}(\text{Nb}_{1-x}\text{Ta}_x)_{0.5}]\text{O}_3$  specimens at various  $x$ : (a)  $x=0$ , (b)  $x=0.2$ , (c)  $x=0.4$ , (d)  $x=0.6$ , (e)  $x=0.8$ , and (f)  $x=1.0$ .Fig. 8. Imaginary part of the dielectric function of  $(\text{Pb}_{0.45}\text{Ca}_{0.55})[\text{Fe}_{0.5}(\text{Nb}_{1-x}\text{Ta}_x)_{0.5}]\text{O}_3$  specimens calculated from Kramers-Kronig analysis: (a)  $x=0$ , (b)  $x=0.2$ , (c)  $x=0.4$ , (d)  $x=0.6$ , (e)  $x=0.8$ , and (f)  $x=1.0$ .

Fig. 6 shows the  $Q_f$  values with the substitution of  $\text{Ta}^{5+}$  ion for  $\text{Nb}^{5+}$  ion. The  $Q_f$  value increased with an increase of  $\text{Ta}^{5+}$  content. In general, the  $Q_f$  value depended on extrinsic factors such as microstructure, secondary phase and density, as well as the intrinsic factor due to lattice anharmonicity.<sup>14</sup> It has been reported that grain size does not significantly affect the  $Q_f$  value.<sup>15,16</sup> The effect of secondary phase might be neglected because there was no secondary phase confirmed in XRD patterns. In addition the effect of density

could be neglected because the relative density of the specimens was above 96%.<sup>9</sup> Therefore, an increase of  $Q \cdot f$  value was related to lattice anharmonicity. The intrinsic behaviour of the specimens was investigated by FT-IR reflectivity spectra.

Fig. 7 shows the IR reflectivity of the specimens denoted by the dotted line, and the calculated values denoted by the solid line. From details of these reflection patterns, such as peak position, half width of peak and peak height, the dielectric constant and dielectric loss could be calculated. From the IR reflectivity spectra, the real part and the imaginary part of the complex dielectric function could be obtained. The imaginary part of complex dielectric function is shown in Fig. 8.

Table 3 summarizes the dispersion parameters obtained from the best fit to the reflectivity data. Twelve phonon modes are available for the best fit of the reflectivity data. The mode contribution to the dielectric constant ( $\Delta\epsilon_j$ ) and dielectric loss ( $\tan \delta_j$ ) denoted by the first mode, was much higher than other mode contributions.

#### 4. Conclusion

The higher bond valence corresponded to the cation with stronger bond strength. This resulted in a lower dielectric constant with increasing Ta<sup>5+</sup> substitution. The TCF of the specimens decreased with tilting of oxygen octahedra due to the increase of the bond valence of the B-site.

From the far-infrared reflectivity spectra, the substitution of Nb<sup>5+</sup> ion by Ta<sup>5+</sup> ion was found to affect the modes contributing to dielectric loss, which resulted in an increase of  $Q \cdot f$  value.

#### Acknowledgements

This work was supported by Korea Research Foundation Grant (KRF-2000-041-E00485).

#### References

1. Brese, N. E. and O'Keeffe, M., Bond-valence parameters for solids. *Acta Crystallogr.*, 1991, **B47**, 192–197.
2. Kim, W. S., Yoon, K. H. and Kim, E. S., Microwave dielectric characteristics of the Ca<sub>2/5</sub>Sm<sub>2/5</sub>TiO<sub>3</sub>-Li<sub>1/2</sub>Nd<sub>1/2</sub>TiO<sub>3</sub> ceramics. *Jpn. J. Appl. Phys.*, 2000, **39**, 5650–5653.
3. Kato, J., Kagata, H., Nishimoto, K. and Inoe, T., Dielectric properties of (PbCa)(MeNb)O<sub>3</sub> at microwave frequencies. *Jpn. J. Appl. Phys.*, 1992, **33**, 3144–3147.
4. Kim, E. S., Choi, W., Yoon, K. H. and Kim, Y., Dielectric properties of (PbCa)(MeNb)((Fe<sub>0.5</sub>Nb<sub>0.5</sub>)<sub>1-x</sub>Ti<sub>x</sub>)O<sub>3</sub> ceramics at microwave frequencies. *Ferroelectrics*, 2001, **257**, 169–174.
5. Kucheiko, S., Choi, Ji-Won, Kim, Hyun-Jai, Yoon, Seok-Jin and Jung, Hyung-Jin, Microwave characteristics of (PbCa)(Fe,Nb,Sn)O<sub>3</sub> dielectric materials. *J. Am. Ceram. Soc.*, 1997, **80**, 240–293.
6. Akbas, M. A. and Davies, P. K., Processing and characterization of lead magnesium tantalate ceramics. *J. Mat. Res.*, 1997, **12**, 2617–2622.
7. Shannon, R. D., Dielectric polarizabilities of ions in oxides and fluorides. *J. Appl. Phys.*, 1993, **73**, 348–366.
8. Hirano, S., Hayashi, T. and Hattori, A., Chemical processing and microwave characteristics of (Zr,Sn)TiO<sub>4</sub> microwave dielectrics. *J. Am. Ceram. Soc.*, 1991, **74**, 1320–1324.
9. Iddles, D. M., Bell, A. J. and Moulson, A. J., Relationships between dopants, microstructure, and the microwave properties of ZrO<sub>2</sub>-TiO<sub>2</sub>-SnO<sub>2</sub> ceramics. *J. Mater. Sci.*, 1992, **27**, 6303–6307.
10. Bosman, A. J. and Havinga, E. E., Temperature dependence of dielectric constants of cubic ionic compounds. *Phys. Rev.*, 1963, **129**, 1593–1600.
11. Colla, E. L., Reaney, I. M. and Setter, N., Effect of structural changes in complex perovskites on the temperature coefficient of the relative permittivity. *J. Appl. Phys.*, 1993, **74**, 3414–3425.
12. Reaney, I. M., Colla, E. L. and Setter, N., Dielectric and structural characteristics of Ba- and Sr-based complex perovskites as a function of tolerance factor. *Jpn. J. Appl. Phys.*, 1994, **33**, 3890–3894.
13. Park, H. S., Yoon, K. H. and Kim, E. S., Relationship between the bond valence and the temperature coefficient of the resonant frequency in the complex perovskite (Pb<sub>1-x</sub>Ca<sub>x</sub>)[Fe<sub>0.5</sub>(Nb<sub>1-y</sub>Ta<sub>y</sub>)<sub>0.5</sub>]O<sub>3</sub>. *J. Am. Ceram. Soc.*, 2001, **84**, 99–103.
14. Kim, W. S., Kim, E. S. and Yoon, K. H., Effect of Sm<sup>3+</sup> substitution on dielectric properties of Ca<sub>1-x</sub>Sm<sub>2x/3</sub>TiO<sub>3</sub> ceramics at microwave frequencies. *J. Am. Ceram. Soc.*, 1999, **82**, 2111–2115.
15. Kawashima, S., Nishida, M., Ueda, I. and Ouchi, H., Ba(Zn<sub>1/3</sub>Ta<sub>2/3</sub>)O<sub>3</sub> ceramics with low dielectric loss at microwave frequencies. *J. Am. Ceram. Soc.*, 1983, **66**(6), 421–423.
16. Liu, P., Kim, E. S. and Yoon, K. H., Low-temperature sintering and microwave dielectric properties of Ca(Li<sub>1/3</sub>Nb<sub>2/3</sub>)O<sub>3-δ</sub> ceramics. *Jpn. J. Appl. Phys.*, 2001, **40**, 5769–5773.